

A new analysis of the short-duration, hard-spectrum GRB 051103, a possible extragalactic soft gamma repeater giant flare

K. Hurley,^{1*} A. Rowlinson,² E. Bellm,¹ D. Perley,³ I. G. Mitrofanov,⁴ D. V. Golovin,⁴ A. S. Kozyrev,⁴ M. L. Litvak,⁴ A. B. Sanin,⁴ W. Boynton,⁵ C. Fellows,⁵ K. Harshmann,⁵ M. Ohno,⁶ K. Yamaoka,⁷ Y. E. Nakagawa,⁸ D. M. Smith,⁹ T. Cline,¹⁰ N. R. Tanvir,² P. T. O'Brien,² K. Wiersema,² E. Rol,^{2,11} A. Levan,¹² J. Rhoads,¹³ A. Fruchter,¹⁴ D. Bersier,¹⁵ J. J. Kavelaars,^{16†} N. Gehrels,¹⁷ H. Krimm,¹⁷ D. M. Palmer,¹⁸ R. C. Duncan,¹⁹ C. Wigger,²⁰ W. Hajdas,²⁰ J.-L. Atteia,²¹ G. Ricker,²² R. Vanderspek,²² A. Rau²³ and A. von Kienlin²³

¹University of California, Space Sciences Laboratory, 7 Gauss Way, Berkeley, CA 94720-7450, USA

²Department of Physics and Astronomy, University of Leicester, University Road, Leicester LE1 7RH

³Department of Astronomy, University of California, Berkeley, CA 94720-3411, USA

⁴Institute for Space Research, Profsojuznaja 84/32, Moscow 117997, Russian Federation

⁵University of Arizona, Lunar and Planetary Laboratory, Tucson, AZ 85721, USA

⁶Institute of Space and Astronautical Science (ISAS/JAXA), 3-1-1 Yoshinodai, Sagami-hara, Kanagawa 229-8510, Japan

⁷Department of Physics and Mathematics, Aoyama Gakuin University, 5-10-1 Fuchinobe, Sagami-hara, Kanagawa 229-8558, Japan

⁸The Institute of Physical and Chemical Research (RIKEN), 2-1 Hirosawa, Wako, Saitama 351-0198, Japan

⁹Department of Physics and Santa Cruz Institute for Particle Physics, University of California, Santa Cruz, 1156 High Street, Santa Cruz, CA 95064, USA

¹⁰Emeritus, NASA Goddard Space Flight Center, Code 661, Greenbelt, MD 20771, USA

¹¹University of Amsterdam, Science Park Amsterdam, Kruislaan 403, 1098 SJ, Amsterdam

¹²Department of Physics, University of Warwick, Coventry CV4 7AL

¹³School of Earth and Space Exploration, Arizona State University, Tempe, AZ 85287, USA

¹⁴Space Telescope Science Institute, 3700 San Martin Drive, Baltimore, MD 21218, USA

¹⁵Astrophysics Research Institute, Liverpool John Moores University, Twelve Quays House, Birkenhead CH41 1LD

¹⁶Herzberg Institute of Astrophysics, National Research Council, 5017 West Saanich Road, Victoria, BC V9E 2E7, Canada

¹⁷NASA Goddard Space Flight Center, Code 661, Greenbelt, MD 20771, USA

¹⁸Los Alamos National Laboratory, PO Box 1663, Los Alamos, NM 87545, USA

¹⁹The University of Texas at Austin, Department of Physics, 1 University Station C1600, Austin, Texas 78712-0264, USA

²⁰Paul Scherrer Institute, CH-5232 Villigen PSI, Switzerland

²¹Laboratoire d'Astrophysique, Observatoire Midi-Pyrénées, 14 avenue E. Belin, 31400 Toulouse, France

²²Kavli Institute for Astrophysics and Space Research, Massachusetts Institute of Technology, 70 Vassar Street, Cambridge, MA 02139, USA

²³Max-Planck-Institut für extraterrestrische Physik, Giessenbachstrasse, Garching 85748, Germany

Accepted 2009 November 25. Received 2009 November 25; in original form 2009 June 24

ABSTRACT

GRB 051103 is considered to be a candidate soft gamma repeater (SGR) extragalactic giant magnetar flare by virtue of its proximity on the sky to M81/M82, as well as its time history, localization and energy spectrum. We have derived a refined interplanetary network localization for this burst which reduces the size of the error box by over a factor of 2. We examine its time history for evidence of a periodic component, which would be one signature of an SGR giant flare, and conclude that this component is neither detected nor detectable under reasonable assumptions. We analyse the time-resolved energy spectra of this event with improved time and energy resolution, and conclude that although the spectrum is very hard its temporal evolution at late times cannot be determined, which further complicates the giant flare association.

*E-mail: khurley@ssl.berkeley.edu

†Visiting Astronomer, Kitt Peak National Observatory, National Optical Astronomy Observatories, which are operated by the Association of Universities for Research in Astronomy, Inc. (AURA) under cooperative agreement with the National Science Foundation.

We also present new optical observations reaching limiting magnitudes of $R > 24.5$, about 4-mag deeper than previously reported. In tandem with serendipitous observations of M81 taken immediately before and 1 month after the burst, these place strong constraints on any rapidly variable sources in the region of the refined error ellipse proximate to M81. We do not find any convincing afterglow candidates from either background galaxies or sources in M81, although within the refined error region we do locate two UV bright star-forming regions which may host SGRs. A supernova remnant (SNR) within the error ellipse could provide further support for an SGR giant flare association, but we were unable to identify any SNR within the error ellipse. These data still do not allow strong constraints on the nature of the GRB 051103 progenitor, and suggest that candidate extragalactic SGR giant flares will be difficult, although not impossible, to confirm.

Key words: stars: neutron – gamma-rays: bursts.

1 INTRODUCTION

Giant flares are the most spectacular manifestations of soft gamma repeaters (SGRs). Their time histories are characterized by a very rapid (< 1 ms) rise to an intense peak lasting several hundred milliseconds, followed by a weaker, oscillatory phase which exhibits the period of the neutron star. The spectrum of the peak is very hard and extends to MeV energies. The most energetic giant flare to date is that of 2004 December 27 from SGR 1806–20, with an isotropic energy of well over 10^{46} erg. (Hurley et al. 2005; Palmer et al. 2005; Mereghetti et al. 2005; Terasawa et al. 2005; Frederiks et al. 2007b). The observation of this event raised the question once more of the existence of extragalactic giant magnetar flares and their relation to the short cosmic gamma-ray bursts (GRBs). Viewed from a large distance, only the initial peak of a giant flare would be detectable, and it would resemble a several hundred millisecond long, hard spectrum GRB. The energetics of giant flares make it a virtual certainty that such events can be detected in distant galaxies, but recognizing them and demonstrating their origin beyond a reasonable doubt remain difficult tasks. Predictions of the rates of extragalactic giant flares, and the percentage of short cosmic bursts which might actually be giant flares, vary widely (from a few to ~ 15 per cent – Lazzati et al. 2005; Nakar et al. 2006; Popov & Stern 2006; Tanvir et al. 2005), in part because of their unknown number–intensity relation (no SGR has yet been observed to emit more than one giant flare, and their distances are uncertain in most cases). However, they generally agree that the rate is small enough that the majority of short bursts are indeed not due to SGR giant flares. On the other hand, the rate is not expected to be zero, so it is important to examine all possible cases exhaustively. In this paper, we revisit GRB 051103, a short burst whose location, time history and energy spectrum are consistent with an origin as a giant flare in M81. We make use of the full interplanetary network (IPN) data set to obtain a refined localization (an error ellipse). We utilize the capability of the Ramaty High Energy Solar Spectroscopic Imager (RHESSI) spacecraft to obtain time-resolved energy spectra with good energy resolution, at a time resolution which is limited only by counting statistics, and we take advantage of the fact that three instruments recorded energy spectra with good statistics to obtain joint fits. Our analysis follows that of Frederiks et al. (2007a), which was based on the Konus–Wind data.

We also present new, much deeper optical data than previously reported for the section of the refined error ellipse closest to M81, taken 3 days after GRB 051103 [and approximately 16 h after the Golenetskii et al. 2005, Gamma-Ray Bursts Coordinates Network

(GCN) notice]. We use these data to search for possible optical counterparts of this short burst [short gamma-ray bursts (SGRB)], and discuss the implications of its non-detection for its progenitor and putative association with M81. Throughout this paper, we utilize the distance modulus of M81 determined by *Hubble Space Telescope* observations of Cepheids, 27.8 (3.6 Mpc; Freedman et al. 1994).

2 IPN OBSERVATIONS AND LOCALIZATION

GRB 051103 occurred at 09:25:42 UT at the Earth, and was observed by the High Energy Transient Experiment French Gamma-Ray Telescope (HETE-FREGATE; Atteia et al. 2003), RHESSI (Smith et al. 2002), *Suzaku*–Wide Area Monitor (WAM; Yamaoka et al. 2009) and *Swift*–Burst Alert Telescope (BAT; Gehrels et al. 2004) in low-Earth orbit; the burst was outside the coded fields of view of *Swift*–BAT and the HETE-II imaging instruments, and was therefore not localized by them. It was also observed by the International Gamma-Ray Astrophysics Laboratory Spectrometer Aboard *INTEGRAL* Anti-Coincidence System (*INTEGRAL* SPI-ACS; Rau et al. 2005) at 0.5 light seconds from the Earth, Konus–Wind (KW; Aptekar et al. 1995) at 4.5 light seconds from the Earth and by Mars Odyssey [the High Energy Neutron Detector (HEND) and the Gamma-Ray Spectrometer (GRS) experiments; Hurley et al. 2006] at 232 light seconds from the Earth. A preliminary IPN error box was announced in a GCN Circular, where it was pointed out that this event had the largest peak flux ever observed by Konus–Wind for a short burst (Golenetskii et al. 2005). Optical followup observations were reported by Lipunov et al. (2005a,b), Klose et al. (2005) and Ofek et al. (2005, 2006), and a radio observation was reported by Cameron & Frail (2005). All yielded negative results. Similarly, a Milagro GeV/TeV observation produced only upper limits (Parkinson 2005).

The observations of each statistically independent spacecraft pair can be analysed to produce an annulus of location, and the annuli can be combined to yield an error ellipse using the method described in Hurley et al. (2000). In this case, we have combined the Konus–HETE, Konus–RHESSI, Konus–*INTEGRAL*, Konus–*Swift*, and Konus–Odyssey annuli. Under these conditions (several relatively short baselines and one relatively long one), the error ellipse has a long major axis, corresponding to the annuli derived from the closer spacecraft pairs, and a short minor axis, corresponding to the annulus from the distant spacecraft pair. We obtain a 3σ error ellipse centred at $\alpha(2000) = 147^{\circ}933$, $\delta(2000) = +68^{\circ}589$, with major and minor axes 137 and 0.96 arcmin, respectively, and

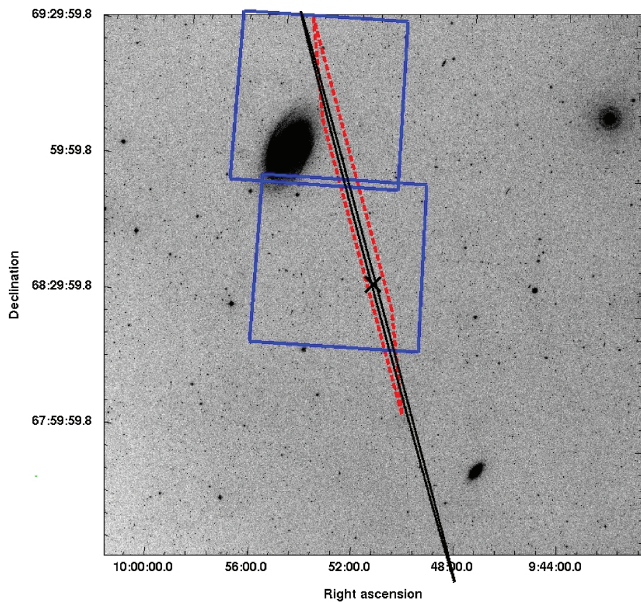


Figure 1. The original IPN error trapezium (dashed line), the 3σ refined error ellipse for the position of GRB 051103 (solid line) and the fields of the region studied using KPNO (large squares). The asterisk indicates the centre of the ellipse and the most likely arrival direction of the burst. Approximately 65 arcmin^2 of the ellipse are contained within the old error box. These are imposed upon an image of the area surrounding M81 from the Digital Sky Survey. The possibility that this burst came from the inner disc of M81 is firmly ruled out. However, the brightest *GALEX* UV knots noted by Ofek et al. (2006) are within the ellipse. Lipunov et al. (2005b) noted the presence of two galaxies within the initial error box, PGC 2719634 and PGC 028505. The former galaxy lies at the 18 per cent confidence contour of the ellipse, and remains a plausible host candidate, while the latter lies at the 0.03 per cent contour, and is unlikely to be the host.

area 104 arcmin^2 . The chi-square for the error ellipse centre is 0.9 for three degrees of freedom (d.o.f.; five annuli minus two fitted coordinates). The area of the initial error box was 240 arcmin^2 .¹ The initial error box and the final error ellipse are shown in Fig. 1.

3 TIME HISTORY

The RHESSI time history of GRB 051103 is shown in the top panel of Fig. 2. A distinctive signature of all three previously observed giant SGR flares within our Galaxy and the Large Magellanic Cloud (LMC) to date is the periodic extended component following the initial short-duration peak. Among these three events, the periods of this extended tail have clustered around a narrow range of 5–8 s and also have a relatively narrow range of total isotropic energy releases of $1\text{--}4 \times 10^{44} \text{ erg}$. This signal lasts for many minutes following the bursts but falls off rapidly after a few hundred seconds. While extended emission is frequently detected following cosmological short-hard bursts, such emission is not periodic. Therefore, detection of a periodic component of emission would be considered a strong confirmation of an SGR origin.

None of the IPN light curves shows obvious evidence for extended emission (pulsed or otherwise) following the burst. However, it is conceivable that a marginally detected signal could be present within the noise. To search for such a component, we acquired *Swift*–BAT data for GRB 051103 (binned at 64 ms) and used the Lomb (1976) periodogram to calculate the relative power in the

¹ A typographical error in GCN 4197 incorrectly gave the area as 120 arcmin^2 .

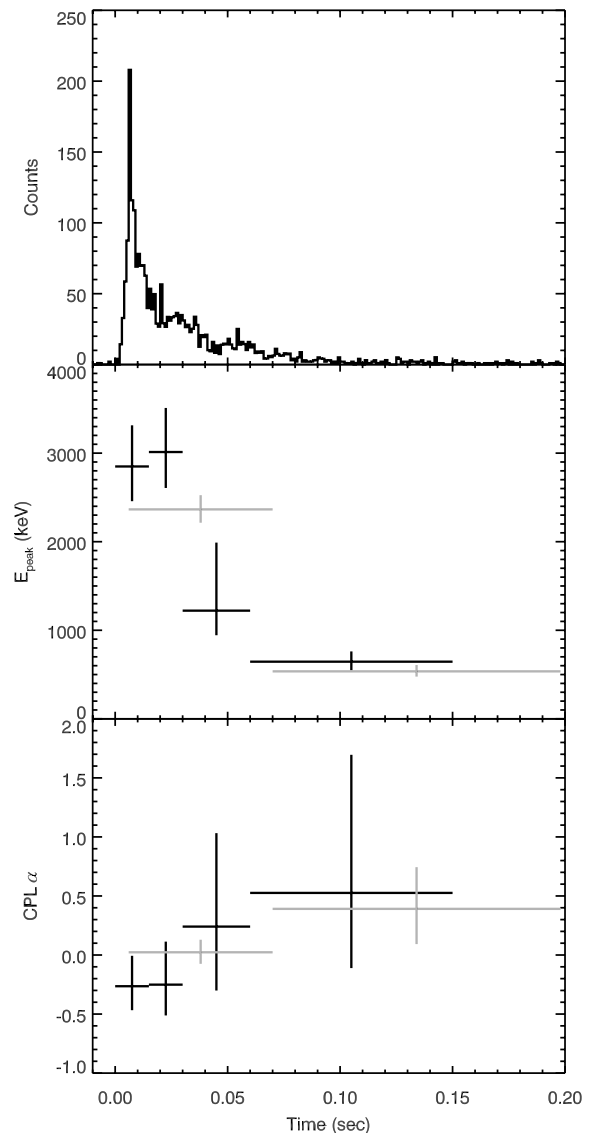


Figure 2. Time history of GRB 051103, and evolution of the spectrum. The top plot shows the dead-time corrected RHESSI light curve (60 keV–3 MeV) with 1-ms time resolution, starting at 09:25:42.184 UT. The background count rate is $0.55 \text{ counts ms}^{-1}$ and has not been subtracted. The time history has an e-folding rise time of $1.2 \pm 0.04 \text{ ms}$, an e-folding decay time of $28.6 \pm 0.6 \text{ ms}$ and a T_{90} of $100 \pm 4 \text{ ms}$. The middle and bottom plots show the evolution of the best-fitting peak spectral energy and power-law index for the CPL model. The black points are RHESSI only, while the grey points are joint fits between RHESSI and Konus-Wind.

signal following the burst at periods up to about 20 s. We created periodograms for all of the four BAT energy channels, which cover the energy range 15–350 keV (and for combinations of channel sums) and for various time ranges following the emission (ranging from the first 60 s to the first 300 s.) To assess the significance of any peaks in the power spectrum, we performed a Monte Carlo analysis by repeatedly randomizing the order of the 64 ms time bins for each data set over the range of interest and measuring the rate of occurrence of independent peaks above various power levels. We identified no peaks with greater than 98 per cent significance in any channel or time range.

This non-detection is expected. To assess the general detectability of periodic post-flare emission from extragalactic giant magnetar

Table 1. Best-fitting parameters for the joint fits of the RHESSI/*Suzaku*–WAM, RHESSI/Konus-Wind and RHESSI-only data.

| Instruments | Interval (s) | E_{peak} (keV) | α | β | RHESSI Fluence (10^{-5} erg cm $^{-2}$) | Normalization offset | $\chi^2/\text{d.o.f.}$ |
|--------------|-----------------|----------------------------|-------------------------|-------------------------|--|---------------------------|------------------------|
| RHESSI + WAM | −0.011 – 0.989 | 2235^{+290}_{-280} | $-0.63^{+0.11}_{-0.09}$ | $-2.59^{+0.07}_{-0.41}$ | $4.80^{+0.23}_{-0.23}$ | $0.196^{+0.013}_{-0.012}$ | 44.7/37 = 1.21 |
| RHESSI + KW | 0.000 – 0.064 | 2080^{+180}_{-200} | $0.13^{+0.14}_{-0.11}$ | $-2.78^{+0.31}_{-0.45}$ | $3.17^{+0.18}_{-0.18}$ | $1.00^{+0.09}_{-0.08}$ | 93.0/65 = 1.43 |
| RHESSI + KW | 0.064 – 0.192 | 536^{+71}_{-59} | $0.39^{+0.35}_{-0.30}$ | – | $0.156^{+0.025}_{-0.024}$ | $1.23^{+0.26}_{-0.20}$ | 30.9/32 = 0.96 |
| RHESSI | −0.006 – 0.009 | 2850^{+465}_{-390} | $-0.26^{+0.26}_{-0.20}$ | – | $1.66^{+0.18}_{-0.18}$ | – | 38.5/11 = 3.50 |
| RHESSI | 0.009 – 0.024 | 3010^{+495}_{-405} | $-0.25^{+0.36}_{-0.26}$ | – | $1.10^{+0.12}_{-0.12}$ | – | 7.5/11 = 0.68 |
| RHESSI | 0.024 – 0.054 | 1220^{+770}_{-280} | $0.24^{+0.79}_{-0.54}$ | – | $0.66^{+1.79}_{-0.18}$ | – | 3.7/4 = 0.93 |
| RHESSI | 0.054 – 0.144 | 645^{+115}_{-95} | $0.53^{+1.17}_{-0.64}$ | – | $0.145^{+0.023}_{-0.022}$ | – | 17.8/7 = 2.54 |

Note. Times are relative to $T_0 = 09:25:42.190$ UT in the RHESSI frame. Joint fit fluences are in the 20 keV–10 MeV band, while the RHESSI-only fluences are 30 keV–10 MeV. The instrument normalizations were free to float in the fit; the normalization of the second instrument relative to RHESSI is given. Errors are quoted at the 90 per cent confidence level.

flares, we also acquired the *Swift*–BAT light curve of the 2004 December 27 flare from SGR 1806–20. We then scaled the signal down by a factor of $(D/D_{\text{SGR}})^2$ and added it to the light curve of GRB 051103 (both scrambled and unscrambled). No signal is detected in the periodogram at the known periodicity of 7.56 s at the distance of M81/82 ($D = 3600$ kpc). The maximum distance for detecting periodicity with our analysis greater than 3σ is only about $D = 220$ kpc (if a distance of $D_{\text{SGR}} = 14.5$ kpc to SGR 1806–20 is assumed, or to 130 kpc if the 8.7 kpc distance of Bibby et al. 2008 is assumed), less than the distance even to M31. This limit may not be exact: both SGR 1806–20 and GRB 051103 were detected off-axis by BAT and the comparative satellite sensitivity will depend on the specifics of the off-axis angle. For the giant flare from 1806–20, BAT was pointing 105° away and slewed to 61° away starting around 38 s after the peak. For 051103, BAT was pointing 122° from the source. However, as the expected signal from a December 27 like event at the distance of M81/M82 would be only 0.01σ assuming similar sensitivities for the two events, we consider it extremely unlikely that any possible angle outside the BAT field of view (FOV) would lead to a detection unless the periodic component was several orders of magnitude stronger than that observed in the three Galactic/LMC events to date.

4 ENERGY SPECTRUM

A key signature of the spectra of the three SGR giant flares observed to date is a very hard energy spectrum for the initial, several hundred millisecond long burst, and a dramatic spectral evolution to a soft spectrum for the subsequent pulsating component. As these bursts were observed by various instruments, with different temporal resolutions, spectral resolutions and energy ranges, and all of them were in some degree of saturation at the peak, a precise description of the spectra is impossible. Nevertheless, all of them can be characterized as very hard spectra at the peak, sometimes consistent with a very high temperature blackbody (e.g. Mazets et al. 1979; Fenimore et al. 1981; Hurley et al. 1999; Mazets et al. 1999; Hurley et al. 2005; Frederiks et al. 2007b). Accordingly, we have analysed the time-resolved energy spectra of GRB 051103. RHESSI, Konus, and *Suzaku* obtained energy spectra for GRB 051103 over a wide energy range, with good statistics, although with different time resolutions. (Due to the off-axis arrival angles at *Swift* and HETE-II, the detector response matrices are not well known, and we have not used these data.) Because the finest time resolution can be obtained from the RHESSI data, we have analysed the RHESSI spectra both separately, to obtain the best time resolution, limited only by count-

ing statistics, and combined with the Konus and *Suzaku* data to obtain the best statistics, albeit at the cost of temporal resolution.

RHESSI uses nine unshielded coaxial germanium detectors to observe a broad energy band (30 keV–17 MeV) with excellent energy (1–5 keV) and time resolution (1 binary μ s) and moderate effective area (~ 150 cm 2). The data are recorded event by event, which provides great flexibility in choosing analysis intervals.

To determine RHESSI’s spectral response to GRB 051103, we used the Monte Carlo package MGEANT (Sturmer et al. 2000). We simulated monoenergetic photons in 192 logarithmic energy bins ranging from 30 keV–30 MeV generated along a 60° azimuthal arc at the 97° off-axis angle of GRB 051103. We fit a polynomial background and extracted the burst data in solarsoftware IDL routine.² Because of radiation damage to some of the detectors, we used only data from rear segments 1, 4, 6, 7 and 8. Spectral fitting was conducted with ISIS v1.4.9 (Houck 2000). In general, the full 30 keV–17 MeV energy band was employed, except when sufficient counts could not be accumulated at high energies.

We fit the data with a Band (Band et al. 1993) function:

$$N_E = \begin{cases} A(E/E_{\text{piv}})^\alpha \exp(-E/E_0) & E < E_{\text{break}} \\ B(E/E_{\text{piv}})^\beta & E > E_{\text{break}} \end{cases}$$

with $E_{\text{break}} \equiv E_0(\alpha - \beta)$ and $B \equiv A[(\alpha - \beta)E_0/E_{\text{piv}}]^{\alpha - \beta} \exp(\beta - \alpha)$. For $\beta < -2$ and $\alpha > -2$, $E_{\text{peak}} \equiv E_0(2 + \alpha)$ corresponds to the peak of the νF_ν spectrum. The normalization A has units photons cm $^{-2}$ s $^{-1}$ keV $^{-1}$ and E_{piv} is here taken to be 100 keV. For joint fits, the Band function parameters α , β and E_{peak} were tied for both instruments, but the normalizations were allowed to vary independently.

For the RHESSI-only time-resolved fits, we identified time intervals with background-subtracted signal-to-noise ratio (S/N) of 20 in the 60 keV–3 MeV band. This yielded three intervals, to which a fourth tail interval of S/N = 12 was added. For most intervals, the cut-off power-law (CPL) model, equivalent to the Band function below E_{break} , provided the best fit. The time evolution of the parameters of the best-fitting spectral model (a CPL model) is presented in the lower panels of Fig. 2. The initial spike of emission has a significantly higher peak energy than the decaying tail; however, the spectral index of the power law appears to harden throughout the burst. The results are reported in Table 1.

Suzaku–WAM did not trigger on GRB 051103, so the only data available are for a 1-s spectrum containing the entire burst, in the 50 keV–5 MeV energy range. The RHESSI–WAM joint fit is shown

² <http://www.lmsal.com/solarsoft/>

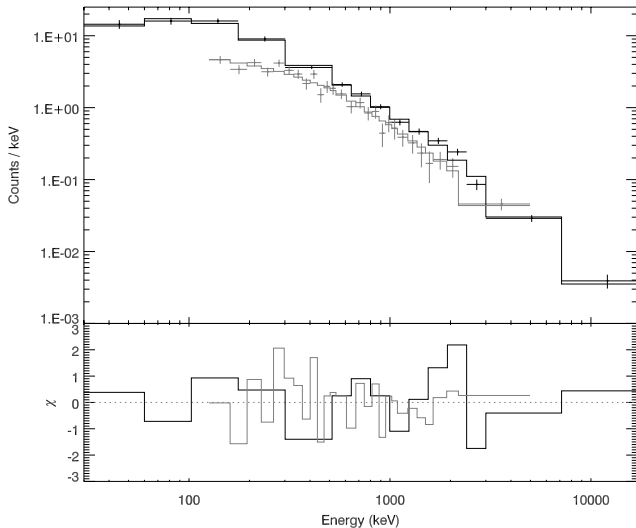


Figure 3. Joint spectral fit of RHESSI (black) and *Suzaku*–WAM (grey) data for a 1-s interval containing the burst.

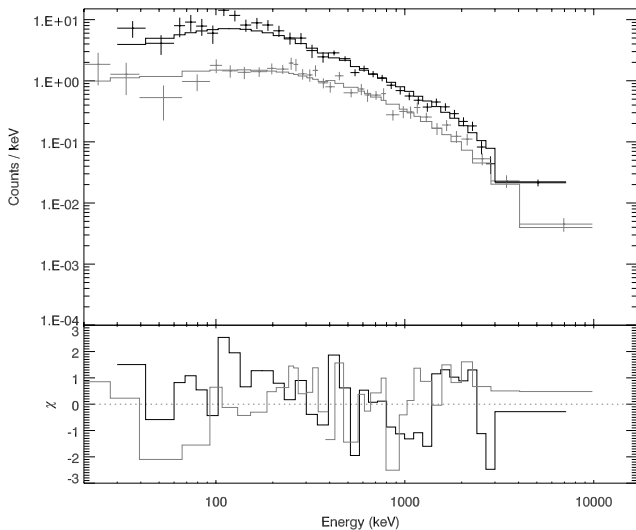


Figure 4. Joint spectral fit of RHESSI (black) and Konus–Wind (grey) data for interval 1. The overplot model is the best-fitting Band function; the normalization between the data sets was allowed to vary in the fit.

in Fig. 3 and the fit results are reported in Table 1. The WAM fluence is a factor of ~ 5 lower than the RHESSI fluence; this deficit appears to be a result of data lost due to dead time during the intense peak of emission.

Konus–Wind triggered on GRB 051103 and recorded 64-ms spectra in the 20 keV–10 MeV range; we conducted joint fits between RHESSI and Konus–Wind for the 64- and 128-ms intervals analysed in Frederiks et al. (2007a). These fits are presented in Figs 4 and 5, and the details are reported in Table 1. Good correspondence was obtained in the best-fitting parameters between the two instruments, although a normalization offset was necessary.

The spectrum of the 2004 December 27 giant flare from SGR 1806–20 was measured by many different instruments, using many different methods (Hurley et al. 2005; Boggs et al. 2007; Palmer et al. 2005; Frederiks et al. 2007b). While they do not agree on the exact shape of the spectrum, none found evidence for the existence of a high-energy power-law component in the Band model. Our RHESSI-only spectral fits of GRB 051103 are consistent with this,

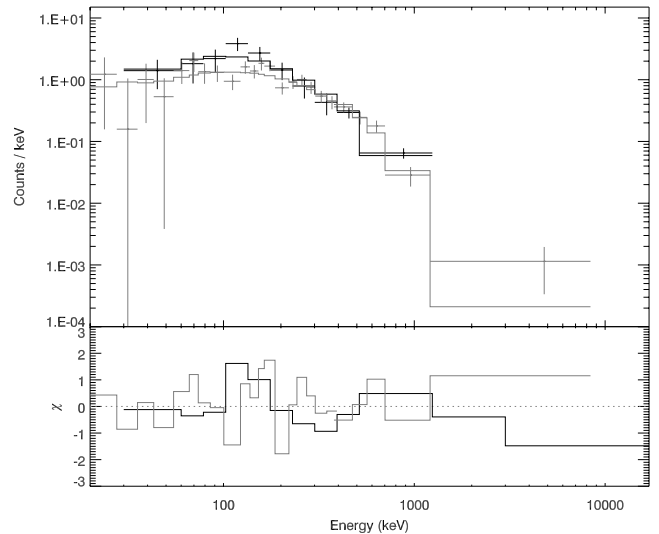


Figure 5. Joint spectral fit of RHESSI and Konus–Wind data for interval 2–3; symbols as in Fig. 4. Two high-energy RHESSI points were negative and are omitted from the logarithmic counts plot.

but in two of the joint fits this component is preferred (Table 1). A blackbody can be fit to the RHESSI data, but only over the 800 keV–5 MeV range; kT is approximately 550 keV for this fit, and the chi-square is about 1.5 per d.o.f.

Table 2 contains a comparison of the energetics of the giant flares observed to date. Because of the uncertainties in the SGR distances, as well as the different energy ranges, time resolutions and characteristics of the various instruments which observed these events, comparisons between the values given are probably uncertain by at least a factor of 3. The total energy of GRB 051103 at the distance of M81, 7.5×10^{46} erg, does not strain the possibilities of the magnetar model. However, PGC 2719634, whose distance is unknown, also remains a possible host (Lipunov et al. 2005b).

5 OPTICAL OBSERVATIONS AND ANALYSIS

Observations were obtained on 2005 November 6 using the Mosaic wide-field optical imaging camera at the Kitt Peak National Observatory (KPNO) 4-m telescope. These data reach a limiting magnitude of ~ 24.5 in the *R* band, which is considerably deeper than the study completed by Ofek et al. (2006). The observations covered the majority of the original error region, and in particular that part nearest to the galaxy M81. The images were flat fielded and sky subtracted using standard tasks within IRAF.³

For comparison, pipeline-reduced images of the region from CFHTLS were obtained via the Virtual Observatory (Walton et al. 2006). These formed part of the wide synoptic survey in the *R* band, also to a limiting magnitude of ~ 25 (Ilbert et al. 2006). Coincidentally, the region was imaged on 2005 November 1, 2 days prior to the burst, and re-imaged within 1 month after the burst. This provided an ideal data set for comparison to the KPNO images as the time-scale between the first images by Canada–France–Hawaii Telescope (CFHT) and our images from KPNO is only 6 days, minimizing any modulation in long-period variable stars in the disc/halo of M81.

³ IRAF is distributed by the National Optical Astronomy Observatories, which are operated by the Association of Universities for Research in Astronomy, Inc., under cooperative agreement with the National Science Foundation.

Table 2. Approximate energies and peak luminosities of the SGR giant flares, and of GRB 051103.

| SGR | Energy (erg) | Peak Luminosity ($\text{erg cm}^{-2} \text{s}^{-1}$) | Assumed distance (kpc) |
|-------------------------|------------------------------|--|------------------------|
| 0525–66 ^a | 1.2×10^{44} | 5×10^{44} | 55 |
| 1900+14 ^b | 4.3×10^{44} | 2×10^{46} | 15 |
| 1806–20 ^c | $2\text{--}5 \times 10^{46}$ | $2\text{--}5 \times 10^{47}$ | 15 |
| GRB 070201 ^d | 1.5×10^{45} | 1.2×10^{47} | 780 |
| GRB 051103 | 7.5×10^{46} | 4.7×10^{48} | 3600 |

^aMazets et al. (1979).^bHurley et al. (1999), Tanaka et al. (2007).^cHurley et al. (2005), Terasawa et al. (2005), Frederiks et al. (2007b).^dMazets et al. (2008).

Fig. 1 shows the previous error quadrilateral, the refined 3σ error ellipse and the fields covered by our KPNO observations, in relation to M81. Our observations were positioned to cover the original error quadrilateral but still cover 62 per cent of the refined 3σ ellipse and contain 76 per cent of the total likelihood. It is important to note that our observations cover the region closest to M81, and therefore our search addresses the possible association of GRB 051103 with M81.

Initially, we searched the images for variability of afterglow counterparts, either at the distance of M81 or in the background, by visual inspection and no obvious afterglow candidate was found. The magnitudes of sources within these images were then studied using SExtractor within *Gaia*. They were all calibrated to the *r*-band magnitudes of stars in the surrounding region as published in the Sloan Digital Sky Survey (SDSS) (Adelman-McCarthy et al. 2008). The *r*-band filter used by CFHT matched the filter used in SDSS and the filter used by KPNO was a Cousins *R*-band filter. Although this is partially taken into account in the calibration to *r*-band magnitudes, there are some sources which have large colour differences, for example very red sources. If a source appeared to differ in magnitude between the CFHT and KPNO images, the colour correction was calculated using a formula developed by Lupton (2005) and it was then determined if the magnitude difference was due to colour effects. If it was not due to colour effects, the source was investigated further. It is important to note that there may be a source within the field which was varying but has not been identified due to this colour correction method. However, this method would only miss objects with a variability of ≤ 0.3 mag (the average colour correction factor used).

Although the magnitude of some stars differed between the images, these were found to be caused by other factors, for example being near chip edges or large diffuse galaxies unidentified by SExtractor. One of the stars in the region studied has a varying magnitude on the images studied and further investigation confirmed it is likely a variable star.

We checked extended sources to look for a conventional SGRB afterglow within a moderately distant host galaxy, with a limiting magnitude of ~ 23.3 . If an extended source appeared to be varying due to a possible point source being superimposed on it, the colour correction was calculated and the object was studied in more depth by eye. This involved using the software to match seeing conditions and measure the size of the object, and then to check if there was an indication of a change in shape which might indicate a superimposed afterglow component.

In addition to the photometry described above, we also searched for afterglow candidates with point spread function matched image subtraction, using a modified version of the ISIS code (Alard & Lupton 1998; Alard 2000). This method gives us a better chance

of finding sources that are blended with other, brighter objects (i.e. bright host galaxies). After cosmic ray cleaning and resampling on a common pixel grid, we subtract the KPNO data with the CFHT data taken before and with the data taken after the burst. We found no credible afterglow candidates.

The analysis of the images found no optical afterglow candidate in the region studied 3 days after GRB 051103. This can place constraints on the progenitor of GRB 051103 by considering the expected results for the potential progenitors.

5.1 Progenitor option 1: a short GRB (SGRB)

The optical afterglows of various SGRBs have been studied and these data can be used to predict the range of afterglow properties of an SGRB of a particular gamma-ray fluence. There is evidence for a reasonable correlation, to first order, between gamma-ray fluence and afterglow flux (Nysewander, Fruchter & Pe'er 2009; Gehrels et al. 2008). Using XSPEC, we created a model spectrum of GRB 051103, using the RHESSI + KW joint fits in Table 1, and estimated the fluence of GRB 051103 in the energy band 15–150 keV to be approximately $9.6^{+14.5}_{-3.7} \times 10^{-7} \text{ erg cm}^{-2}$.

It is possible to compare GRB 051103 to other SGRBs in the BAT catalogue (Sakamoto et al. 2008) using the approximate fluence, calculated for the energy band 15–150 keV, and the photon indices given in Table 1. GRB 051103 is isolated at the extreme bright, hard end of the SGRBs in the *Swift* distribution (cf. fig. 14 from Sakamoto et al. 2008). Similarly, in the study of short bursts by Mazets et al. (2004) over the much wider Konus energy range, of the 109 spectra which could be characterized by an E_{peak} , none exceeded 2.53 MeV. The peak energy of GRB 051103 is approximately 3 MeV (table 1). Thus, if GRB 051103 is an SGRB rather than an SGR giant flare it is a fairly extreme case.

We compared the fluence of this burst to other SGRBs observed by the *Swift* Satellite. Table 3 provides the data of SGRB with fluences in the band 15–150 keV and late optical observations, obtained from the relevant GCNs, and measured optical afterglows in the *R* band, approximately 3 days after each burst.⁴ For two of the bursts, it was necessary to estimate the fluence in the correct energy band using the same method as with GRB 051103. This is not a complete sample of SGRBs, as there are a number with a relatively low gamma-ray fluence that were either not observed optically, were not observed for longer than a few hours or did not have a detected optical afterglow. We chose this sample so we did not have to rely on the assumption that we can extrapolate the light curve to later epochs and because they are of a similar gamma-ray fluence to GRB

⁴ It is important to note the classification of some of these SGRBs are currently being debated (Zhang et al. 2009).

Table 3. The observed fluence, in the energy band 15–150 keV, of SGRBs with observed *R*-band magnitudes at approximately 3 d.

| SGRB | Fluence (10^{-7} erg cm $^{-2}$) | <i>R</i> -band magnitude at 3 d |
|---------|---|---------------------------------|
| 051221A | 11.6 ± 0.4^1 | 24.12 ± 0.28^2 |
| 051227 | 2.3 ± 0.3^3 | 25.49 ± 0.09^4 |
| 060121 | $26.7^{+5.3}_{-20.2}^5$ | 25 ± 0.25^6 |
| 060614 | 217 ± 4^7 | 22.74 ± 0.31^8 |
| 061006 | 14.3 ± 1.4^9 | $>23.96 \pm 0.12^{10}$ |
| 070707 | $0.334^{+0.753}_{-0.316}^{11}$ | 26.62 ± 0.18^{12} |
| 070714B | 7.2 ± 0.9^{13} | $<25.5^{14}$ |
| 071227 | 2.2 ± 0.3^{15} | $>24.9^{16}$ |
| 080503 | 20.0 ± 1^{17} | 25.90 ± 0.23^{18} |

¹Cummings et al. (2005); ²Soderberg et al. (2006); ³Hullinger et al. (2005); ⁴D’Avanzo et al. (2009); ⁵an approximate fluence calculated using spectral parameters published by Golenetskii et al. (2006); ⁶based on observations by Levan et al. (2006a); ⁷Barthelmy et al. (2006); ⁸Mangano et al. (2007); ⁹Krimm et al. (2006); ¹⁰an upper limit based on observations 2 days after the burst completed by D’Avanzo et al. (2009); ¹¹an approximate fluence calculated using spectral parameters published by Golenetskii et al. (2007); ¹²Piranomonte et al. (2008); ¹³Barbier et al. (2007); ¹⁴a lower limit based on observations 4 days after the burst completed by Perley et al. (2009); ¹⁵Sato et al. (2007); ¹⁶a 3σ upper limit published by D’Avanzo et al. (2009); ¹⁷Ukwatta et al. (2008); ¹⁸Perley et al. (2009).

051103. We compared the SGRBs in Table 3 to GRB 051103 and predict the optical afterglow would have an *R*-band magnitude of ~ 24 as it is at the higher end of the fluence distribution. This is within the limiting magnitude of the KPNO and CFHTLS images used, but would have been unobservable in the images obtained by Ofek et al. (2006). As no afterglow was observed, this rules out most typical SGRBs in the region of the error ellipse covered by our imaging. However, there are cases of SGRBs with extremely faint optical afterglows, for example GRB 080503, which had a similar fluence to GRB 051103 and an *r*-band magnitude of 25.90 ± 0.23 at 3 d (Perley et al. 2009). So the observations cannot rule out an unusually faint SGRB in this region similar to GRB 080503. Additionally, GRB 051103 could be a classical SGRB in the part of the error ellipse not studied in this paper.

5.2 Progenitor option 2: an SGR giant flare in M81

Conversely, GRB 051103 could be an SGR giant flare in M81 with similar energy to the giant flare from SGR 1806–20 (Golenetskii et al. 2005) and a very faint optical afterglow (Eichler 2002; Levan et al. 2008). Using observations of the giant flare from SGR 1806–20, we can predict the apparent optical magnitude of an SGR in M81. The distance to SGR 1806–20 has proven difficult to determine; the distance modulus adopted by many authors is 15.8 (Corbel et al. 1997), although Bibby et al. (2008) recently obtained a revised distance modulus estimate of 14.7 ± 0.35 mag. Here, we continue to use the larger distance modulus as this will provide an approximate upper limit on the absolute magnitude. The giant flare from SGR 1806–20 had an observed radio afterglow and this has been used by Wang et al. (2005) to make predictions of the apparent *R*-band magnitude of the afterglow. Their analysis suggests that the giant flare would have had an apparent magnitude of ~ 22 at 3 d, and hence an absolute magnitude of $M \approx 6$. Taking this as the absolute magnitude of any afterglow of GRB 051103 if it is an SGR giant flare, and using the distance modulus to M81 of 27.8 (Freedman et al. 1994), we conclude the afterglow would

be expected to have an apparent magnitude of >34 . Despite the many uncertainties involved in this calculation, we can have some confidence that such an afterglow would not be detectable with the data available. For future reference, it is important to note that with more accurate positions and rapid follow up observations it may be possible to observe the optical afterglows of extragalactic giant flares. For example, if there were a second potential giant flare in M81 we predict the optical afterglow would have a peak apparent *K*-band magnitude of ~ 20 at 86 s after the giant flare and would fall to ~ 26 at 1 h. This is observable with current and upcoming facilities, for example the European Extremely Large Telescope. However, these predictions are based upon the theoretical models of SGR giant flares being similar to the blast wave model used to describe classical GRBs. Wang et al. (2005) use the blast wave model and radio observations of the giant flare from SGR 1806–20 to extrapolate the optical afterglow. SGRs have been observed during periods of activity using Robotic Optical Transient Search Experiment 1 (ROTSE-I) (Akerlof et al. 2000) and *Swift* (e.g. Cummings et al. 2009), and infrared observations have been obtained for SGR 1900+14 4.1 days after outburst detecting no variability (Oppenheimer et al. 1998). These have provided upper limits on the optical afterglows from the softer spectrum, shorter and weaker bursts seen during active phases of SGRs, but it is important to note that there have been no reported rapid optical followup observations of galactic SGR giant flares, which have a significantly higher fluence and are spectrally harder than these bursts. Therefore, we are completely reliant on theoretical predictions, and future observations may show discrepancies with these predictions. Indeed, our observations with a limiting magnitude of 24.5, giving an absolute magnitude -3.3 assuming it is at a distance of 3.6 Mpc, constitute one of the deepest absolute magnitude searches for an afterglow from a possible SGR giant flare. This absolute magnitude is only exceeded by the search for an afterglow from GRB 070201, which is a candidate SGR giant flare in M31, corresponding to an absolute magnitude of -7.4 obtained 10.6 h after the burst (Ofek et al. 2008). However, as we discuss later, it is unlikely that both of these events were SGR giant flares (Chapman, Priddey & Tanvir 2009).

From the *Galaxy Evolution Explorer* (GALEX) UV imaging (Martin et al. 2005), there is evidence that the error ellipse does contain star-forming regions in the outer disc of M81. The two brightest UV sources are marked in Fig. 6 (Ofek et al. 2006). These young stellar regions in M81 could host an SGR which could emit a giant flare. Similarly, these UV regions could be the locations of massive star clusters, and SGRs 1900+14 and 1806–20 have been associated with massive star clusters (Mirabel, Fuchs & Chaty 2000; Vrba et al. 2000). However, if GRB 051103 is an SGR giant flare in M81, we might also expect to find a young (up to $\sim 10^4$ year old; Duncan & Thompson 1992) supernova remnant (SNR) in the nearby region, although this association is still being debated (Gaensler et al. 2001, 2005). When an SGR is formed, it is theoretically possible that it is given a kick of up to 1000 km s^{-1} or more (Duncan & Thompson 1992) and therefore could have travelled a distance of $>10 \text{ pc}$ from the SNR. However, this is only equivalent to an angular separation of $\sim 0.6 \text{ arcsec}$ at a distance of 3.6 Mpc (Freedman et al. 1994). Hence, an accompanying SNR would still be expected to fall within the error ellipse. Of the known SNR in M81 (Matonick & Fesen 1997), there is none within the error ellipse.

M81 has been studied by the *Chandra X-Ray Observatory* (Swartz et al. 2003) and three X-ray sources are within the error ellipse. However, they have not been identified in visible or radio observations. Additionally, they have not been identified with

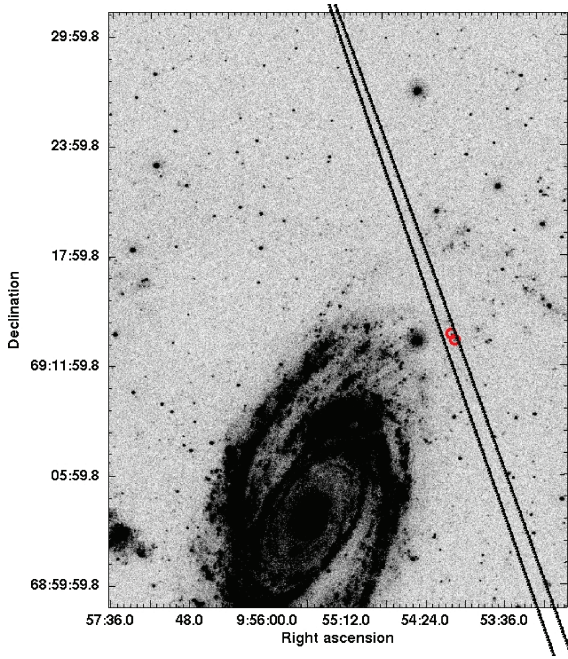


Figure 6. GALEX image showing the UV sources within the error ellipse. Two of the brightest sources discussed by Ofek et al. (2006) are highlighted by the circles within the ellipse.

known SNR, nearby stars, are not co-incident with H II star-forming regions (the expected location of SGRs – Duncan & Thompson 1992) and are more likely to be X-ray binary systems than unidentified SNR (Swartz et al. 2003). This survey had a limiting luminosity of $3 \times 10^{36} \text{ erg s}^{-1}$, which means it would detect very young supernovae, as the oldest supernovae with detected X-ray afterglows had a luminosity of $\sim 10^{37} \text{ erg s}^{-1}$ and an age of ~ 60 years (Soria & Perna 2008). Additionally, this survey would detect the X-ray luminous SNR as these have a luminosity of up to $\sim 10^{37} \text{ erg s}^{-1}$ but would not detect the X-ray faint SNRs which have a luminosity of $\sim 10^{34} \text{ erg s}^{-1}$ (Immler & Kuntz 2005). SGRs are well known to be quiescent soft X-ray emitters and Mereghetti et al. (2000) have measured the soft X-ray flux of SGR 1806–20 to be approximately $10^{-11} \text{ erg cm}^{-2} \text{ s}^{-1}$. Frederiks et al. (2007a) determined that the *Chandra Observatory* would be unable to observe directly the persistent X-ray flux from an SGR like SGR 1806–20 in M81.

An alternative method of searching for SNR is to use H α and O III narrow-band observations. The Isaac Newton Telescope (INT) has been used to search for planetary nebulae in M81 by Magrini et al. (2001) and they have found 171 potential candidates, some of which are in the nearby region of the refined error ellipse. Their criteria for differentiating between an SNR and a planetary nebula is that planetary nebulae cannot be spatially resolved and SNR are resolvable. A young SNR, as required for an SGR, could be misidentified as a planetary nebula by this criterion, since a 1-arcsec region corresponds to a physical size of $\sim 20 \text{ pc}$. Young SNRs may well be significantly smaller than this, since an expansion velocity of a few thousand km s^{-1} over a magnetar lifetime of $\sim 10^4$ years leads to sizes of 10–50 pc. Indeed, many SNRs in M82 appear (based on radio maps) to be fairly compact (Fenech et al. 2008). However, the nearest is still $\sim 23 \text{ arcsec}$ from the error ellipse, and we showed earlier that an SGR in M81 would only be able to travel $\sim 0.6 \text{ arcsec}$ from its birthplace. The H α luminosity of SNRs in nearby disc galaxies tends to be greater than $\sim 10^{36} \text{ erg s}^{-1}$ (de Grijs et al. 2000) and the work by Magrini et al. (2001) had a limiting H α flux of

less than $6 \times 10^{-17} \text{ erg cm}^{-2} \text{ s}^{-1}$ which corresponds to a limiting luminosity of $\sim 10^{35} \text{ erg s}^{-1}$. Therefore, we would expect their survey to find a candidate SNR. We used the recently published H α and O III images from the INT Wide Field Camera Imaging Survey (McMahon et al. 2001), with a limiting luminosity of $\sim 10^{35} \text{ erg s}^{-1}$ at the distance of M81 as these are the same images as used by Magrini et al. (2001), and compared them with 21-cm radio images from The HI Nearby Galaxy Survey (THINGS) (Walter et al. 2008) and *Chandra* X-ray source positions (Swartz et al. 2003) to search for previously unidentified SNRs within the error ellipse. There is a possible circular 21-cm radio source coincident with a *Chandra* X-ray source of approximately the right flux for an SNR in M81 (source 15 in Swartz et al. 2003). However, the 21-cm radio source is too large for an SNR of the required age and there is no convincing supporting evidence of a source within the other images studied. Using the published known X-ray sources, we might have expected to find an SNR if it was very young or bright and would have expected to find an associated SNR using the H α images. We identified no convincing associated SNR candidates within the error ellipse.

Although it has been determined that the error ellipse does cross potential star formation regions as required by the majority of SGR models, it should also be noted that this is not essential for all. An alternative route has been proposed for producing a magnetar by white dwarf (WD) mergers (King, Pringle & Wickramasinghe 2001; Levan et al. 2006b). As WD have long lifetimes, WD–WD mergers would be associated with older populations of stars. It is possible that accretion induced collapse (AIC) will drive off a fraction of the envelope, leaving something akin to an SNR behind (e.g. Baron et al. 1987). The mechanisms underlying AIC are poorly understood, and the physical characteristics and detectability of such remnants are not clear. Therefore, a SGR produced through this channel could be formed in an old stellar population within the outer disc or halo, and the non-detection of an SNR within the region does not place constraints on this model.

If the progenitor was an SGR giant flare then there might be significant similarities in the light curve and spectrum of GRB 051103 to the giant flare from SGR 1806–20. Ofek et al. (2006) noted that the light curve of these two events were consistent, i.e. the light curve of GRB 051103 is similar to what would be expected from an extragalactic version of the giant flare from SGR 1806–20. In Table 1, we have shown, for the joint RHESSI + KW fits, that initially $\alpha = 0.13^{+0.14}_{-0.11}$ and softens to $\alpha = 0.39^{+0.35}_{-0.30}$. Although this is unusually hard for a GRB, it is consistent with the photon index of the giant flare from SGR 1806–20, $\alpha = 0.2 \pm 0.3$ (Palmer et al. 2005). The peak luminosity of GRB 051103, assuming it was from an SGR in M81, is approximately $4.7 \times 10^{48} \text{ erg s}^{-1}$. This is a factor of 10 brighter than the peak luminosity of the giant flare from SGR 1806–20, which is $2\text{--}5 \times 10^{47} \text{ erg s}^{-1}$ assuming it is at a distance of 15 kpc (Hurley et al. 2005). With the revised distance estimate from Bibby et al. (2008), the peak luminosity of the giant flare from SGR 1806–20 would be $7 \times 10^{46} \text{ erg s}^{-1}$, suggesting that a much smaller percentage of SGRBs is SGR giant flares. This value is 30 times fainter than the peak luminosity of GRB 051103 if it was from an SGR giant flare in M81 and in this case GRB 051103 would be the most luminous SGR giant flare observed. In comparison, the peak luminosity of GRB 070201 is $1.14 \times 10^{47} \text{ erg s}^{-1}$ assuming it was in M31 (Ofek et al. 2008), which is an order of magnitude fainter than GRB 051103 and comparable to the giant flare from SGR 1806–20. It is important to note, however, that there is currently no theoretical upper limit for the energy of a giant flare. Duncan & Thompson (1992) showed that the total energy available is given

by $E \propto 3 \times 10^{47} B_{15}^2 \text{ erg}$ where $B_{15} = B/10^{15} \text{ G}$. Therefore, the magnetic dipole (B) of SGR 1806–20 would only need to increase by a factor of ~ 5 to produce a giant flare with an energy that is 30 times greater than the one from SGR 1806–20.

Although the gamma-ray data suggest that GRB 051103 may be an extragalactic SGR giant flare, it is important to note that SGR giant flares are rare events. Considering plausible luminosity functions, Chapman et al. (2009) calculated the probability that the IPN would observe a giant flare, with energy greater than the energy emitted by the giant flare from SGR 1806–20, in the region surveyed during the 17 years it has operated. For one giant flare, they calculated the probability to be 10 per cent. However, as we discussed in the introduction, there are four potential candidates for extragalactic SGR giant flares, including GRB 070201 near M31 which has been identified as an SGR giant flare by Mazets et al. (2008). The probability that the IPN has detected two SGR giant flares, with energy greater than the giant flare from SGR 1806–20, is 0.6 per cent (Chapman et al. 2009). Recently, several new SGR candidates have been identified including 0501+4516, 1550–5418 and possibly 0623–0006 (Barthelmy et al. 2008a; Krimm et al. 2008; Barthelmy et al. 2008b), which may imply that the number of SGRs in the Milky Way is higher than previously thought. In this case, the luminosity of the giant flare from SGR 1806–20 would have to be at the peak of the luminosity function of SGR giant flares and therefore giant flares of this luminosity must be extremely rare events. This argues that GRB 051103 is unlikely to be a second SGR giant flare in the nearby Universe.

6 CONCLUSIONS

GRB 051103 illustrates the difficulties of identifying a short burst as an extragalactic giant magnetar flare beyond a reasonable doubt. Even setting aside the questions of detecting and localizing such events, and establishing their associations with nearby galaxies, their interpretation is problematic. On the one hand, the localization, short duration and hard energy spectra of GRB 051103 suggest that it is a giant flare from M81. However, a deeper analysis of its time history demonstrates that the periodic component, which is a key signature of giant flares, is unlikely to ever be detected at great distances by the IPN if all giant flares are similar to the three observed to date. The energy spectrum at the peak of the emission is very hard ($E_{\text{peak}} \sim 3 \text{ MeV}$), and is detected to 7 MeV at the 3σ level, with marginal emission up to 17 MeV. Yet it is not inconceivable that a short-duration GRB could have these properties. Although the E_{peak} of GRB 051103 evolves from hard to soft, the evolution to a very soft spectrum, which is expected during the oscillatory phase of an SGR giant flare, is undetectable, as is the oscillatory phase itself. Thus, evidence for an extragalactic giant flare origin of GRB 051103 remains tantalizing, but inconclusive. On a more positive note, if an extragalactic magnetar flare occurred within the *Swift*–BAT FOV, so that the X-ray Telescope could begin observing within a minute or so, the periodic component would be detectable at low energies to at least 10 Mpc (Hurley et al. 2005).

We have presented new optical observations of GRB 051103 and have determined that there is no *R*-band optical afterglow with a limiting magnitude of ~ 24.5 (for an afterglow overlapping a host galaxy, the limiting magnitude is ~ 23.3) in the region of the error ellipse covered by our observations. Comparison of the prompt emission of GRB 051103 with a sample of other SGRBs leads us to conclude that if it was a classical SGRB we would expect to have located an optical afterglow in our observations.

In contrast, if GRB 051103 were an SGR giant flare in M81, non-detection of an afterglow would not be surprising as the expectations for optical afterglow emission lie significantly below the limits obtained here, or the limits likely to be attained via current technology. The case for an SGR origin would be strengthened if there were an accompanying SNR within the error ellipse, but there is no evidence of this. An SGR produced via AIC of a WD (Levan et al. 2006b) would, however, remove the requirement for an SNR. Additionally, the luminosity of GRB 051103, assuming it is from an SGR giant flare in M81, is significantly higher than known SGR giant flares but still attainable with current theoretical models. Giant flares with luminosity similar to the giant flare from SGR 1806–20 are extremely rare and it is unlikely that GRB 051103 and GRB 070201 are both extragalactic SGR giant flares.

Although we have not considered this option in detail, it is possible that the progenitor of GRB 051103 was a compact binary merger in M81. In this case, it would just be within the reach of current gravitational wave searches. This scenario was ruled out at >99 per cent confidence for GRB 070201 in M31 using the Laser Interferometer Gravitational-wave Observatory (LIGO) observations, and distances out to 3.5 Mpc were ruled out to 90 per cent confidence (Abbott et al. 2008). The LIGO Scientific Collaboration is currently considering a search for gravitational-wave signals in the data surrounding GRB 051103 (Jones and Sutton, private communication).

ACKNOWLEDGMENTS

KH is grateful for IPN support from the NASA Guest Investigator programmes for *Swift* (NASA NNG04GQ84G), INTEGRAL (NAG5-12706) and *Suzaku* (NNX06AI36G); for support under the Mars Odyssey Participating Scientist Program, JPL Contract 1282046 and under the HETE-II co-investigator program, MIT Contract SC-A-293291. We are also grateful to the Konus–Wind team – E. Mazets, S. Golenetskii, D. Frederiks, V. Pal’shin and R. Aptekar – for contributing the Konus data to this study.

AR, KW and ER, NRT and AL would like to acknowledge funding from the Science and Technology Funding Council.

This research has made use of data obtained using, or software provided by, the UK’s AstroGrid Virtual Observatory Project, which is funded by the Science and Technology Facilities Council and through the EU’s Framework 6 programme.

The National Optical Astronomy Observatory (NOAO) consists of Kitt Peak National Observatory near Tucson, Arizona, Cerro Tololo Inter-American Observatory near La Serena, Chile and the NOAO Gemini Science Centre. NOAO is operated by the Association of the Universities for Research in Astronomy under a cooperative agreement with the National Science Foundation.

Based on observations with MegaPrime/MegaCam, a joint project of CFHT and CEA/DAPNIA, at the CFHT which is operated by the National Research Council (NRC) of Canada, the Institut National des Sciences de l’Univers of the Centre National de la Recherche Scientifique (CNRS) of France and the University of Hawaii. This work is based in part on data products produced at TERAPIX and the Canadian Astronomy Data Centre as part of the CFHT Legacy Survey, a collaborative project of NRC and CNRS.

The Digitized Sky Surveys were produced at the Space Telescope Science Institute under US Government grant NAG W-2166. The images of these surveys are based on photographic data obtained using the Oschin Schmidt Telescope on Palomar Mountain and the UK Schmidt Telescope. The plates were processed into the present compressed digital form with the permission of these institutions.

Based on observations made through the Isaac Newton Group's Wide Field Camera Survey Programme with the INT operated on the island of La Palma by the Isaac Newton Group in the Spanish Observatorio del Roque de los Muchachos of the Instituto de Astrofísica de Canarias.

This work made use of 'THINGS' (Walter et al. 2008).

We also acknowledge useful discussions with G. Jones and P. Sutton.

REFERENCES

- Abbott B. et al., 2008, *ApJ*, 681, 1419
 Adelman-McCarthy J. K. et al., 2008, *ApJS*, 175, 297
 Akerlof C. et al., 2000, *ApJ*, 542, 251
 Alard C., 2000, *A&AS*, 144, 363
 Alard C., Lupton R. H., 1998, *ApJ*, 503, 325
 Aptekar R. et al., 1995, *Space Sci. Rev.*, 71, 265
 Atteia J.-L. et al., 2003, in Ricker G., Vanderspek R., eds, *AIP Conf. Proc.* 662, *Gamma-Ray Burst and Afterglow Astronomy – A Workshop Celebrating the First Year of the HETE Mission*. AIP, New York, p. 17
 Band D. et al., 1993, *ApJ*, 413, 281
 Barbier L. et al., 2007, *GCN Circ.*, 6623, 1
 Baron E., Cooperstein J., Kahana S., Nomoto K., 1987, *ApJ*, 320, 304
 Barthelmy S. et al., 2006, *GCN Circ.*, 5256, 1
 Barthelmy S. D. et al., 2008a, *GCN Circ.*, 8113, 1
 Barthelmy S. D. et al., 2008b, *GCN Circ.*, 8458, 1
 Bibby J. L., Crowther P. A., Furness J. P., Clark J. S., 2008, *MNRAS*, 386, L23
 Boggs S. et al., 2007, *ApJ*, 661, 458
 Cameron P., Frail D., 2005, *GCN Circ.*, 4266
 Chapman R., Priddey R. S., Tanvir N. R., 2009, *MNRAS*, 395, 1515
 Corbel S., Wallyn P., Dame T. M., Durouchoux P., Mahoney W. A., Vilhu O., Grindlay J. E., 1997, *ApJ*, 478, 624
 Cummings J. et al., 2005, *GCN Circ.*, 4365, 1
 Cummings J. R., Page K. L., Beardmore A. P., Gehrels N., 2009, *ATel*, 2127, 1
 D'Avanzo P. et al., 2009, *A&A*, 498, 711
 de Grijs R., O'Connell R. W., Becker G. D., Chevalier R. A., Gallagher J. S., III, 2000, *AJ*, 119, 681
 Duncan R. C., Thompson C., 1992, *ApJ*, 392, L9
 Eichler D., 2002, *MNRAS*, 335, 883
 Fenech D. M., Muxlow T. W. B., Beswick R. J., Pedlar A., Argo M. K., 2008, *MNRAS*, 391, 1384
 Fenimore E., Evans W., Klebesadel R., Laros J., Terrell J., 1981, *Nat*, 289, 42
 Frederiks D. D., Palshin V. D., Aptekar R. L., Golenetskii S. V., Cline T. L., Mazets E. P., 2007a, *Astron. Lett.*, 33, 19
 Frederiks D. D., Palshin V. D., Aptekar R. L., Golenetskii S. V., Cline T. L., Mazets E. P., 2007b, *Astron. Lett.*, 33, 1
 Freedman W. L. et al., 1994, *ApJ*, 427, 628
 Gaensler B. M., Slane P. O., Gotthelf E. V., Vasisht G., 2001, *ApJ*, 559, 963
 Gaensler B. M., McClure-Griffiths N. M., Oey M. S., Haverkorn M., Dickey J. M., Green A. J., 2005, *ApJ*, 620, L95
 Gehrels N. et al., 2004, *ApJ*, 611, 1005
 Gehrels N. et al., 2008, *ApJ*, 689, 1161
 Golenetskii S., Aptekar R., Mazets E., Pal'Shin V., Frederiks D., Cline T., 2007, *GCN Circ.*, 6615, 1
 Golenetskii S., Aptekar R., Mazets E., Pal'Shin V., Frederiks D., Cline T., 2006, *GCN Circ.*, 4564, 1
 Golenetskii S. et al., 2005, *GCN Circ.*, 4197, 1
 Houck J., 2000, in Manset N., Veillet C., Crabtree D., eds, *ASP Conf. Ser.* Vol. 216, *Astronomical Data Analysis Software and Systems IX*. Astron. Soc. Pac., San Francisco, p. 591
 Hullinger D. et al., 2005, *GCN Circ.*, 4400, 1
 Hurley K. et al., 1999, *Nat*, 397, 41
 Hurley K. et al., 2000, *ApJ*, 537, 953
 Hurley K. et al., 2005, *Nat*, 434, 1098
 Hurley K. et al., 2006, *ApJS*, 164, 124
 Ilbert O. et al., 2006, *A&A*, 457, 841
 Immler S., Kuntz K. D., 2005, *ApJ*, 632, L99
 King A. R., Pringle J. E., Wickramasinghe D. T., 2001, *MNRAS*, 320, L45
 Klose S., Ferrero P., Kann D. A., Steklum B., Laux U., 2005, *GCN Circ.*, 4207
 Krimm H. et al., 2006, *GCN Circ.*, 5704, 1
 Krimm H. A., Beardmore A. P., Gehrels N., Page K. L., Palmer D. M., Starling R. L. C., Ukwatta T. N., 2008, *GCN Circ.*, 8312, 1
 Lazzati D., Ghirlanda G., Ghisellini G., 2005, *MNRAS*, 362, L8
 Levan A. J. et al., 2006a, *ApJ*, 648, L9
 Levan A. J., Wynn G. A., Chapman R., Davies M. B., King A. R., Priddey R. S., Tanvir N. R., 2006b, *MNRAS*, 368, L1
 Levan A. J. et al., 2008, *MNRAS*, 384, 541
 Lipunov V. et al., 2005a, *GCN Circ.*, 4198
 Lipunov V. et al., 2005b, *GCN Circ.*, 4206
 Lomb N., 1976, *Astrophys. Space Sci.*, 39, 447
 Lupton R., 2005, <http://www.sdss.org/dr7/>
 McMahon R. G., Walton N. A., Irwin M. J., Lewis J. R., Bunclark P. S., Jones D. H., 2001, *New Astron. Rev.*, 45, 97
 Magrini L., Perinotto M., Corradi R. L. M., Mampaso A., 2001, *A&A*, 379, 90
 Mangano V. et al., 2007, *A&A*, 470, 105
 Martin D. C. et al., 2005, *ApJ*, 619, L1
 Matonick D. M., Fesen R. A., 1997, *ApJS*, 112, 49
 Mazets E. P. et al., 1979, *Nat*, 282, 587
 Mazets E. P. et al., 1999, *Astron. Lett.*, 25, 635
 Mazets E. P., Cline T. L., Aptekar R. L., Butterworth P. S., Frederiks D. D., Golenetskii S. V., Il'Inskii V. N., Pal'shin V. D., 2004, in Feroci M., Frontera F., Masetti N., Piro L., eds, *ASP Conf. Ser.* Vol. 312, *Proc. of the Third Rome Workshop on Gamma-Ray Bursts in the Afterglow Era*. Astron. Soc. Pac., San Francisco, p. 102
 Mazets E. P. et al., 2008, *ApJ*, 680, 545
 Mereghetti S., Cremonesi D., Feroci M., Tavani M., 2000, *A&A*, 361, 240
 Mereghetti S., Götz D., von Kienlin A., Rau A., Lichti G., Weidenspointner G., Jean P., 2005, *ApJ*, 624, L105
 Mirabel I. F., Fuchs Y., Chaty S., 2000, in Kippen R. M., Mallozzi R. S., Fishman G. J., eds, *AIP Conf. Proc.* Vol. 526, *Gamma-Ray Bursts*, 5th Huntsville Symposium. Am. Inst. Phys., New York, p. 814
 Nakar E., Gal-Yam A., Piran T., Fox D., 2006, *ApJ*, 640, 849
 Nysewander M., Fruchter A. S., Pe'er A., 2009, *ApJ*, 701, 824
 Ofek E. O., Cenko S. B., Soderberg A. M., Kulkarni S. R., Fox D. B., 2005, *GCN Circ.*, 4208
 Ofek E. O. et al., 2006, *ApJ*, 652, 507
 Ofek E. O. et al., 2008, *ApJ*, 681, 1464
 Oppenheimer B. R., Bloom J. S., Eikenberry S. S., Matthews K., 1998, *ATel*, 26, 1
 Palmer D. M. et al., 2005, *Nat*, 434, 1107
 Parkinson P., 2005, *GCN Circ.*, 4249
 Perley D. A. et al., 2009, *ApJ*, 696, 1871
 Piranomonte S. et al., 2008, *A&A*, 491, 183
 Popov S., Stern B., 2006, *MNRAS*, 365, 885
 Rau A., Kienlin A. V., Hurley K., Lichti G. G., 2005, *A&A*, 438, 1175
 Sakamoto T. et al., 2008, *ApJS*, 175, 179
 Sato G. et al., 2007, *GCN Circ.*, 7148, 1
 Smith D. M. et al., 2002, *Solar Phys.*, 210, 33
 Soderberg A. M. et al., 2006, *ApJ*, 650, 261
 Soria R., Perna R., 2008, *ApJ*, 683, 767
 Sturmer S. J., Seifert H., Shrader C., Teegarden B. J., 2000, in McConnell M. L., Ryan J. M., eds, *AIP Conf. Ser.* Vol. 510, *The Fifth Compton Symposium*. Am. Inst. Phys., New York, p. 814
 Swartz D. A., Ghosh K. K., McCollough M. L., Pannuti T. G., Tennant A. F., Wu K., 2003, *ApJS*, 144, 213
 Tanaka Y. T., Terasawa T., Kawai N., Yoshida A., Yoshikawa I., Saito Y., Takashima T., Mukai T., 2007, *ApJ*, 665, L55
 Tanvir N. R., Chapman R., Levan A. J., Priddey R. S., 2005, *Nat*, 438, 991

- Terasawa T. et al., 2005, *Nat*, 434, 1110
 Ukwatta T. et al., 2008, *GCN Circ.*, 7673, 1
 Vrba F. J., Henden A. A., Luginbuhl C. B., Guetter H. H., Hartmann D. H., Klose S., 2000, *ApJ*, 533, L17
 Walter F., Brinks E., de Blok W. J. G., Bigiel F., Kennicutt R. C., Thornley M. D., Leroy A., 2008, *AJ*, 136, 2563
 Walton N. A., Richards A. M. S., Padovani P., Allen M. G., 2006, in Whitelock P. A., Dennefeld M., Leibundgut B., eds, *Proc. IAU Symp.* 232, *The Scientific Requirements for Extremely Large Telescopes (ELTs)*. Cambridge Univ. Press, Cambridge, p. 398
 Wang X. Y., Wu X. F., Fan Y. Z., Dai Z. G., Zhang B., 2005, *ApJ*, 623, L29
 Yamaoka K. et al., 2009, *PASJ*, 61, S35
 Zhang B. et al., 2009, *ApJ*, 703, 1696

This paper has been typeset from a \TeX/L\TeX file prepared by the author.